

- (33) L. J. Vande Griend, J. G. Verkade, J. F. M. Pennings, and H. M. Buck, *J. Am. Chem. Soc.*, **99**, 2459 (1977).
- (34) B. L. Laube, R. D. Bertrand, G. A. Casedy, R. D. Compton, and J. G. Verkade, *Inorg. Chem.*, **6**, 173 (1967).
- (35) J. C. Clardy, R. L. Kolpa, and J. G. Verkade, *Phosphorus*, **4**, 133 (1974).
- (36) This procedure is essentially that given by P. Nicpon and D. W. Meek, *Inorg. Synth.*, **10**, 157 (1967), for the preparation of phosphine selenides from KSeCN.
- (37) D. S. Milbrath, J. G. Verkade, D. H. Eargle, and G. L. Kenyon, *J. Am. Chem. Soc.*, **100**, 3167 (1978).
- (38) For reasons discussed elsewhere (ref 33) the trend in $^1J(^1\text{H}-^{31}\text{P})$ does not exactly follow that in $\nu(\text{BH})$ and hence not in $^1J(^{77}\text{Se}-^{31}\text{P})$. Thus the first two members of the series are reversed: $\text{HP}(\text{OMe})_3^+ < \mathbf{1b} < \mathbf{1a} < \mathbf{2} < \mathbf{3} < \mathbf{4}$ (where H^+ replaces Se in 1-4).
- (39) J. A. Mosbo and J. G. Verkade, *J. Org. Chem.*, **9**, 1549 (1977).
- (40) F. A. Cotton and G. Wilkinson, "Advanced Inorganic Chemistry", Interscience, New York, 1972.
- (41) R. T. Sanderson, "Inorganic Chemistry", Reinhold, New York, 1967.
- (42) A. S. Tarasevich and Yu. P. Egerov, *Theor. Exp. Chem. (Engl. Transl.)*, **7**, 676 (1971).

Contribution from the Inorganic Chemistry Research Laboratories, Imperial College of Science and Technology, London SW7 2AY, United Kingdom

Electron Spin Resonance Study of Manganese(II) Ions in Trigonal-Prismatic Coordination in Tris(acetylacetonato)metal(II) Anions

ROSHUN B. BIRDY and MARGARET GOODGAME*

Received July 27, 1978

ESR spectra are reported for manganese(II) ions doped into polycrystalline $\text{M}^{\text{I}}[\text{M}^{\text{II}}(\text{acac})_3] \cdot n\text{H}_2\text{O}$ ($\text{M}^{\text{I}} = \text{Na, K; M}^{\text{II}} = \text{Co, Ni, Zn, Cd}$). Zero-field splitting parameters D and λ ($=E/D$) are derived, and the results are correlated with the distortions of the anions from octahedral geometry. For the cadmium compounds, the high values of D are consistent with trigonal-prismatic geometry, for $\text{K}[\text{M}(\text{acac})_3]$ ($\text{M} = \text{Co, Ni}$) the results indicate near-octahedral structures, while for $\text{Na}[\text{M}(\text{acac})_3] \cdot n\text{H}_2\text{O}$ ($\text{M} = \text{Co, Ni, Zn}$) intermediate values are obtained.

Introduction

In recent years ESR has been shown^{1,2} to be a useful tool in determining the stereochemistry of manganese(II) complexes. Moreover, some attempts have been made to use this ion as a stereochemical probe for other divalent metal ions.^{3,4} However, no investigations appear to have been made of the ESR spectra of manganese(II) ions in trigonal-prismatic coordination, in spite of the growing recognition of this geometry as a viable alternative to the octahedron in certain cases.

We report here an ESR study of manganese(II) ions doped into polycrystalline $\text{K}[\text{Cd}(\text{acac})_3]\text{H}_2\text{O}$, which has recently been shown to have trigonal-prismatic geometry.⁵ Further studies with other tris(acetylacetonato) anions as host lattices have been made for comparison.

Experimental Section

The complexes were prepared by the method of Dwyer and Sargeson⁶ and had satisfactory analyses. The doping was 1% nominal, and the complexes were magnetically dilute. Attempts to prepare $\text{K}[\text{Zn}(\text{Mn})(\text{acac})_3]$ were unsuccessful.

All spectra were obtained on polycrystalline samples at room temperature. The spectrometers have been described previously.⁷

Spectral Results

Spectra were obtained at X- and Q-band for each of the doped complexes. The results were interpreted using the "simplified" spin-Hamiltonian (1) in which A and g are as-

$$\mathcal{H} = g\beta BS + D(S_z^2 - \frac{1}{3}S^2) + E(S_x^2 - S_y^2) + SAI \quad (1)$$

sumed isotropic, with $g = 2.00$. A first estimate for the values of D and E was made using first-order perturbation theory. The values were then refined by exact diagonalization of a spin Hamiltonian matrix based on (1) but omitting the hyperfine interaction term. The calculated energy levels were scanned using the program⁷ ESRs.

The X-band spectrum of $\text{K}[\text{Cd}(\text{Mn})(\text{acac})_3]\text{H}_2\text{O}$ was exceedingly complicated, with a large number of overlapping transitions. The better resolution at Q-band was therefore necessary to an interpretation of the results. A good fit to this spectrum was obtained using the parameters $D = 0.113 \text{ cm}^{-1}$ and λ ($=E/D$) = 0.06 (Table I). Similar assignment at

Table I. Q-Band ESR Spectrum (mT) of $\text{K}[\text{Cd}(\text{Mn})(\text{acac})_3] \cdot \text{H}_2\text{O}$

obsd ($\nu = 35.85 \text{ GHz}$)	calcd for $D = 0.113 \text{ cm}^{-1}$, $\lambda = 0.06$	
	B	axis, levels ^a
796 w	797	a_z
1005 ms	1009	e_y
1036 ms	1039	b_z
1085 ms	1098	e_x
1124 s	1129	d_y
1167 s	1168	d_x
1354 s	1361	b_x
1405 s	1408	b_y
1487 ms	1489	a_x
1517 ms	1522	d_z
1572 ms	1574	a_y
1764 w	1765	e_z

^a Assignments are for negative D ; see text.

Table II. Q-Band ESR Spectrum (mT) of $\text{Na}[\text{Cd}(\text{Mn})(\text{acac})_3]$

obsd ($\nu = 35.815 \text{ GHz}$)	calcd for $D = 0.109 \text{ cm}^{-1}$, $\lambda = 0.03$	
	B	axis, levels ^a
828 w	813	a_z
1035 ms	1038	e_y
	1046	b_z
1085 ms	1081	e_x
1138 s	1143	d_y
1159 s	1162	d_x
1374 s	1369	b_x
1390 s	1391	b_y
1501 ms	1501	a_x
	1513	d_z
1532 ms	1541	a_y
	1746	e_z

^a Assignments are for negative D .

X-band is less useful, on account of both the serious overlapping of transitions and the mixing of wave functions, which occurs here.

The "best-fit" parameters from the Q-band spectrum were therefore used to simulate the random-orientation X-band

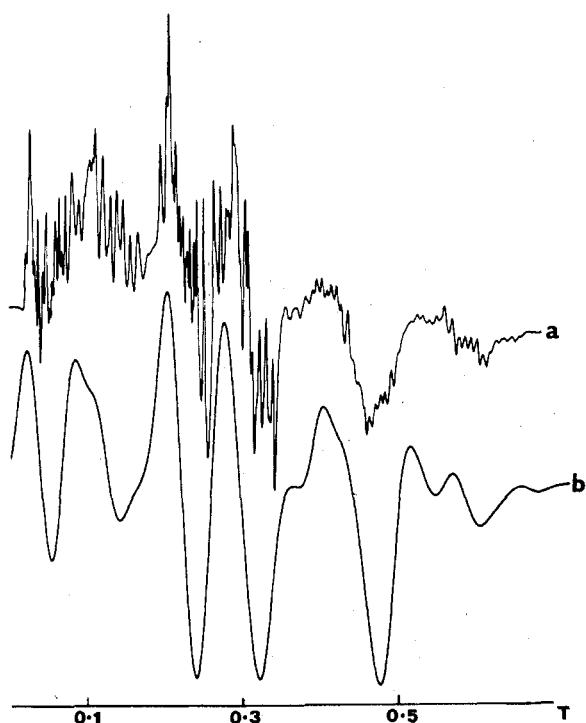


Figure 1. ESR spectrum ($\nu = 9.531$ GHz, 0–700 mT) of $\text{K}[\text{Mn}(\text{acac})_3] \cdot \text{H}_2\text{O}$: (a) experimental values; (b) calculated for $D = 0.113 \text{ cm}^{-1}$, $\lambda = 0.06$, $\Delta B_{pp} = 30$ mT.

spectrum, excluding hyperfine splitting, using the program⁸ SHAPE 9. A Gaussian line shape was assumed, with an isotropic peak-to-peak line width of the first-derivative spectrum of 30 mT. A comparison of the experimental and calculated spectra is given in Figure 1.

Study of a similar host lattice with sodium as the counterion showed the Q-band spectrum to be qualitatively similar to that of the potassium salt. However, slightly decreased band separation indicated lower values of D and λ , and the best fit (Table II) was obtained for $D = 0.109 \text{ cm}^{-1}$ and $\lambda = 0.03$. Simulation of the X-band spectrum using these parameters again gave good agreement with the observed spectrum.

In the $[\text{Co}(\text{acac})_3]^-$ and $[\text{Ni}(\text{acac})_3]^-$ lattices, with potassium as the counterion, very much simpler spectra were obtained, with only one well-resolved transition, at $g_{\text{eff}} = 2$. The resolution of the hyperfine components shows that this is not due to magnetic concentration, and it appears that in these two compounds the distortion is very much less, and $D < 0.02 \text{ cm}^{-1}$. No value of λ could be assessed.

For the sodium salts of the cobalt, nickel, and zinc host anions, which are mutually isomorphous, the spectral profiles are very similar to one another and also to those of manganese(II) in the hexakis(4-methylpyridine *N*-oxide) complexes of zinc, cadmium, and mercury.⁴ For the nickel complex, however, line widths were greater and the spectra were generally less well resolved, especially at Q-band frequency. From the $\Delta M_S = \pm 1$ lines, the axial zero-field parameter is calculated to be about 0.06 cm^{-1} in all three complexes, and λ is 0. For the cobalt and zinc complexes the best fit was obtained for $D = 0.063 \text{ cm}^{-1}$, while for the nickel complex, where transitions with $B \parallel z$ were not resolved, the D value is 0.060 cm^{-1} (Tables III–V).

With D of this magnitude, the sign of the splitting may be determined from the spacing of the hyperfine components of the $\pm^{3/2} \leftrightarrow \pm^{5/2}$ transitions with B parallel to z . This spacing was greater for the lowest allowed transition (a_z of Table III) than for the highest band (e_z). Values of A calculated for the two bands were 8.7 mT (0.0081 cm^{-1}) and 8.3 mT (0.0078 cm^{-1}), respectively. Assuming that A is negative, as is usually

Table III. X-Band ESR Spectrum (mT) of $\text{Na}[\text{M}(\text{Mn})(\text{acac})_3] \cdot n\text{H}_2\text{O}$ ($M = \text{Co}, \text{Zn}$)

obsd ($\nu = 9.532$ GHz)	calcd for $D = -0.063 \text{ cm}^{-1}$, $\lambda = 0$	
	B	axis, levels
68	70.6	a_z
121	a	
126	a	
	205.6	b_z
224	225.9	$e_{x,y}$
265	265.8	$d_{x,y}$
316	317.0	$c_{x,y}$
384	383.7	$b_{x,y}$
475	475.4	d_z
482	483.0	$a_{x,y}$
612	610.4	e_z

^a Assigned as spin-forbidden transitions. See Table VI and text.

Table IV. Q-Band ESR Spectrum (mT) of $\text{Na}[\text{M}(\text{Mn})(\text{acac})_3] \cdot n\text{H}_2\text{O}$ ($M = \text{Co}, \text{Zn}$)

obsd ($\nu = 35.44$ GHz)	calcd for $D = -0.063 \text{ cm}^{-1}$, $\lambda = 0$	
	B	axis, levels
993	996	a_z
1131	1131	b_z
	1135	$e_{x,y}$
1190	1195	$d_{x,y}$
1328	1328	$b_{x,y}$
1403	1401	d_z
	1404	$a_{x,y}$
1534	1536	e_z

Table V. X-Band ESR Spectrum^a (mT) of $\text{Na}[\text{Ni}(\text{Mn})(\text{acac})_3] \cdot 0.5\text{H}_2\text{O}$

obsd ($\nu = 9.527$ GHz)	calcd for $D = -0.060 \text{ cm}^{-1}$, $\lambda = 0$	
	B	axis, levels
229	230.0	$e_{x,y}$
268	269.0	$d_{x,y}$
316	318.6	$c_{x,y}$
474	475.9	$a_{x,y}$

^a Transitions for $B \parallel z$ not resolved.

the case for manganese(II), the lowest transition is $-5/2 \leftrightarrow -3/2$, and D is negative. A negative sign for D has been assumed, by analogy, for the cadmium complexes, since in these cases severe overlapping of transitions in the X-band spectra precluded an experimental determination of the sign. If this assumption is wrong, the assignments a–e of Tables I and II would have to be reversed.

The sharp bands between 100 and 160 mT in $\text{Na}[\text{Co}(\text{Mn})(\text{acac})_3] \cdot 0.5\text{H}_2\text{O}$ and $\text{Na}[\text{Zn}(\text{Mn})(\text{acac})_3] \cdot \text{H}_2\text{O}$ are assigned as “spin-forbidden” ($\Delta M_S \neq \pm 1$) bands. This region shows irregular hyperfine structure, which is shown (Table VI) to be due to the overlapping of components in three different transitions. The intensity of the absorption in this region (Figure 2) shows the importance of such transitions in powder spectra, even though their single-crystal transition probabilities are low.

At the particular value of the zero-field splitting found in these compounds, the behavior of the 6–3 transition is calculated to show an interesting dependence on the sign of the zero-field splitting. For negative D , the $\Delta M_I = 0$ lines should be strongest, although their transition probabilities are only about half of the calculated value in the absence of nuclear hyperfine interaction. When D is positive, however, transitions which are formally nuclear allowed have negligible probability, while the “ $\Delta M_I = \pm 1$ ” lines become weakly allowed. It is doubtful, however, whether this effect could be seen unambiguously in the experimental spectrum, because of the severe

Table VI. $\Delta M_s \neq 1$ Transitions (100–160 mT) in the X-Band Spectrum of $\text{Na}[\text{M}(\text{Mn})(\text{acac})_3] \cdot n\text{H}_2\text{O}$ ($\text{M} = \text{Co}, \text{Zn}$)

obsd ($\nu = 9.532$ GHz)	calcd for $D = -0.063 \text{ cm}^{-1}$, $\lambda = 0$, $A = -9.1 \text{ mT}$		
	5–2 transition ^a $\theta = 30^\circ$, $\Delta M_I = 0$	4–2 transition ^a $\theta = 75^\circ$, $\Delta M_I = 0$	6–3 transition ^a $\theta = 90^\circ$, $\Delta M_I = 0$
101.6 s	101.8 (0.66) ^b [$-5/2$] ^c		101.6 (0.54) [$1/2$] ^d
105.7 m		106.2 (0.19) [$-5/2$]	
109.3 m	109.5 (0.33) [$-3/2$]		
114.0 s		114.1 (0.19) [$-3/2$]	
117.6 m	117.9 (0.28) [$-1/2$]		
		122.4 (0.19) [$-1/2$]	120.2 (0.56) [$3/2$] ^d
126.9 m	127.1 (0.34) [$1/2$]		
132.1 s		131.3 (0.19) [$1/2$]	
			133.2 (0.32) [$5/2$] ^d
137.2 m	137.1 (0.49) [$3/2$]		
		140.9 (0.20) [$3/2$]	
^e			
148.1 s	148.1 (0.78) [$5/2$]		
151.2 m		151.1 (0.21) [$5/2$]	

^a Because of severe mixing of wave functions, the spin levels are labeled 1–6 in order of decreasing energy. ^b Transition probability in parentheses. ^c M_I in square brackets. ^d Some “mixing” of nuclear levels occurs. ^e Strong but poorly resolved absorption.

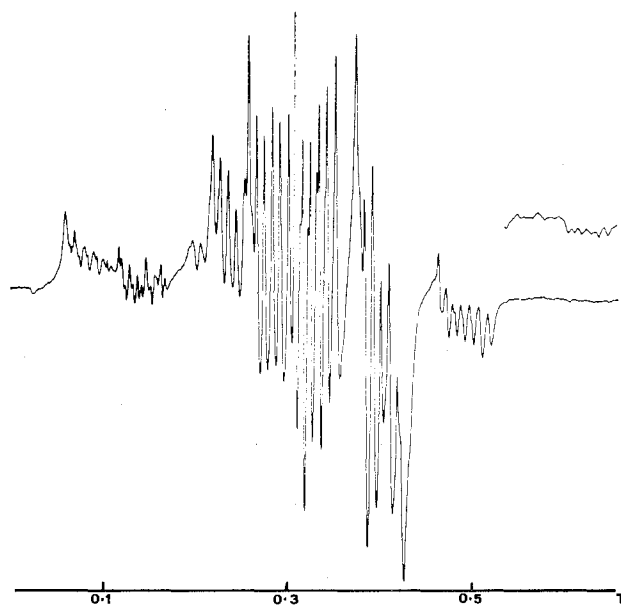


Figure 2. ESR spectrum ($\nu = 9.532$ GHz) of $\text{Na}[\text{Zn}(\text{Mn})(\text{acac})_3] \cdot \text{H}_2\text{O}$.

overlapping of the components of the 6–3 transition with those of the 4–2 and 5–2 transitions (Table VI).

Discussion

The spectra are readily interpreted in terms of the spin Hamiltonian (1) and the hyperfine interaction is of the magnitude expected for manganese(II) with little delocalization of the unpaired electrons. Although, therefore, the trigonal-prismatic $\text{K}[\text{Cd}(\text{acac})_3] \cdot \text{H}_2\text{O}$ shares some of the structural characteristics of the tris(dithiolenes), the manganese here shows none of the highly unusual magnetic properties of those complexes.

The compression ratio s/h in this complex, calculated from the crystallographic data⁵ and the expressions of Stiefel and Brown,⁹ is 1.04, compared with 1.22 for a regular octahedron. That elongation of this magnitude does not in itself contribute significantly to the zero-field splitting is illustrated by the results for the isomorphous hexakis(antipyrine) complexes¹⁰ of $\text{Mg}(\text{II})$, $\text{Ca}(\text{II})$, and $\text{Pb}(\text{II})$, each doped with $\text{Mn}(\text{II})$ (Table VII). The increase in magnitude of D from the $\text{Pb}(\text{II})$ to the $\text{Mg}(\text{II})$ complex reflects the decrease in cation size of the host lattice which clearly more than compensates for the effect on the zero-field splitting of the concomitant progression from trigonally elongated to regular octahedral geometry.¹¹

Table VII. Structural and ESR Data for Some Hexakis(antipyrine) Complexes

complex	s/h^a	D (10^{-4} cm^{-1}) of $\text{Mn}(\text{II})$ impurity ^b	ionic radius (Å) of host metal ion
$\text{MgL}_6(\text{ClO}_4)_2$	1.23	-44.4	0.66
$\text{CaL}_6(\text{ClO}_4)_2$	1.17	-32.0	0.99
$\text{PbL}_6(\text{ClO}_4)_2$	1.09	-8.7	1.20

^a Calculated from the values of h/x ($x =$ centroid to apex distance of a triangular face) cited in ref 11. ^b Data from ref 10.

It must also be considered whether the potassium ions, one of which lies directly on the threefold axis of the complex anion, could contribute significantly to the zero-field splitting. Sharma¹² has calculated the zero-field splitting arising from the presence of two unit positive charges on opposite sides of a threefold axis of cubic symmetry, and at a distance of $4a_0$ ($=2.12 \text{ Å}$) from the manganese(II) ion, as -0.0268 cm^{-1} . Since the K–Cd distance in $\text{K}[\text{Cd}(\text{acac})_3] \cdot \text{H}_2\text{O}$ is 3.94 Å, the contribution to D from this source would appear to be very small, though these calculations have been criticized,¹³ and the results could be invalidated by neglect of the relativistic crystal field effect.

It seems likely, then, that trigonal-prismatic coordination in the anion is responsible for the remarkably high axial distortion in this compound; D is well in excess of any previously reported for a MnO_6 chromophore. Recent crystal field calculations for the d^5 configuration¹⁴ suggest that trigonal elongation of an octahedron should give rise to a negative value of D , and negative values have been found for the hexakis(antipyrine) complexes¹⁰ (Table VII). The small rhombic distortion is to be expected in view of the inequalities in the Cd–O bond lengths (which vary from 2.247 to 2.325 Å) and in the angles subtended at the metal by the donor atoms.

No crystallographic information is available for the other complexes. However, the similarity of the EPR spectra suggests that the $[\text{Cd}(\text{acac})_3]^-$ complex has very similar geometry in the potassium and sodium salts. The stabilization of the trigonal-prismatic arrangement in the potassium salt has been attributed⁵ to the interaction of the acetylacetonate oxygens with the monovalent cations, thus giving a chain structure. It is not clear, however, why this arrangement is more stable than one involving chains of octahedra. What seems likely is that metal–ligand interaction energies are similar in the two geometries, as calculated from both valence-bond theory¹⁵ and ab initio and extended Hückel MO

theory.¹⁶ The reduction in interligand repulsion by removal of electron density on the oxygen atoms may then be sufficient to overcome the usual strong preference for octahedral geometry.

The MO calculation¹⁶ suggested that the trigonal prism should have slightly higher stability than the octahedron for a d^{10} ion, though this was considered to be an artefact of the method of calculation. However, it would be expected that the tendency to octahedral geometry would increase where crystal field effects enhance its stability. It is not surprising, therefore, that $K[M(acac)_3]$ ($M = Co$ and Ni) apparently have geometries close to octahedral. It seems, however, that with the stronger polarizing power of sodium cations, there may be an appreciable trigonal twist of the octahedron, since the D values are again very high for six identical donor atoms.

It is clear that the EPR signal of manganese(II) ions doped into the lattice gives a very sensitive method of detecting such deviations from idealized geometry. However, far more investigations on compounds of known structure are required in order to provide a basis for their interpretation. From the present work it seems likely that the observed negative value of D corresponds to a trigonally elongated arrangement of donor atoms, and, particularly, to a low value of the twist angle ϕ .⁹

Acknowledgment. We thank the University of London for a Postgraduate Studentship (to R.B.B.) and Dr. J. F. Gibson for the use of computer programs.

Registry No. $K[Cd(acac)_3]$, 68566-67-6; $Na[Cd(acac)_3]$, 68566-68-7; $Na[Co(acac)_3]$, 20106-06-3; $Na[Zn(acac)_3]$, 14589-37-8; $Na[Ni(acac)_3]$, 42230-53-5; $Mn(II)$, 16397-91-4.

References and Notes

- (1) R. D. Dowsing, J. F. Gibson, D. M. L. Goodgame, M. Goodgame, and P. J. Hayward, *Nature (London)*, **219**, 1037 (1968).
- (2) C. J. O'Connor and R. L. Carlin, *Inorg. Chem.*, **14**, 291 (1975).
- (3) M. Goodgame and P. J. Hayward, *J. Chem. Soc. A*, 3406 (1971).
- (4) R. B. Birdy and M. Goodgame, *J. Chem. Soc., Dalton Trans.*, 461 (1977).
- (5) T. M. Greaney, C. L. Raston, and A. H. White, *J. Chem. Soc., Dalton Trans.*, 876 (1975).
- (6) F. P. Dwyer and A. M. Sargeson, *J. Proc. R. Soc. N.S.W.*, **40**, 29 (1956).
- (7) D. Vivien and J. F. Gibson, *J. Chem. Soc., Faraday Trans. 2*, 1640 (1975).
- (8) J. F. Gibson and G. M. Lack, to be submitted for publication.
- (9) E. I. Stiefel and G. F. Brown, *Inorg. Chem.*, **11**, 434 (1972).
- (10) G. M. Woltermann and J. R. Wasson, *J. Phys. Chem.*, **77**, 945 (1973).
- (11) M. Vijayan and M. A. Viswamitra, *Acta Crystallogr., Sect. B*, **24**, 1067 (1968).
- (12) R. R. Sharma, *Phys. Rev. B*, **3**, 76 (1971).
- (13) R. Chatterjee, M. R. Smith, and H. A. Buckmaster, *Can. J. Phys.*, **54**, 1224 (1976).
- (14) J. C. Hempel, *J. Chem. Phys.*, **64**, 4307 (1976).
- (15) R. Hultgren, *Phys. Rev.*, **40**, 891 (1932).
- (16) R. Hoffmann, J. M. Howell, and A. R. Rossi, *J. Am. Chem. Soc.*, **98**, 2484 (1976).

Contribution from the Chemistry Department and Energy and Mineral Resources Research Institute, Iowa State University, Ames, Iowa 50011, and the Chemistry Department, Auburn University, Auburn, Alabama 36830

Polarized Electronic Absorption Spectra for Dirhodium(II) Tetraacetate Dihydrate

DON S. MARTIN, JR.,*^{1a} THOMAS R. WEBB,^{1b} GARY A. ROBBINS,^{1a} and PHILLIP E. FANWICK^{1a}

Received July 7, 1978

Single-crystal polarized absorption spectra are reported for the $\bar{1}01$ face of $Rh_2(O_2CCH_3)_4 \cdot 2H_2O$ in the region of 15 500–30 000 cm^{-1} and at temperatures of 300 and 15 K. An absorption band with a maximum at 17 300 cm^{-1} possesses vibrational structure in the $\perp b$ polarization. It corresponds to molecular x,y polarization and has been assigned as $Rh-Rh \pi^* \rightarrow Rh-Rh \sigma^*$. Weaker absorptions with maxima at 23 300 cm^{-1} in $\perp b$ and 22 200 cm^{-1} in $\parallel b$ indicate the presence of more than one transition in this region. Possible assignments for these transitions are discussed.

Introduction

Polarized electronic absorption spectra have been reported in recent years for a number of dimeric complexes of molybdenum²⁻⁵ and rhenium^{6,7} which possess multiple metal-metal bonds. The present work provides polarized spectra recorded at temperatures of ca. 300 and 15 K for single crystals of $Rh_2(O_2CCH_3)_4 \cdot 2H_2O$. Norman and Kolari⁸ have recently completed an $X\alpha$ scattered-wave computation for ground-state orbital energies of anhydrous and hydrated dirhodium(II) tetraacetate, and they have reviewed rather well conflicting claims in the literature concerning the existence of a single or multiple rhodium-rhodium bond in this molecule. The crystal structure for the $Rh_2(O_2CCH_3)_4 \cdot 2H_2O$ is available from the X-ray diffraction study of Cotton et al.⁹ The visible absorption bands of $Rh_2(O_2CCH_3)_4$ in H_2O as well as in a series of basic solvents have been listed by Johnson, Hunt, and Neuman.¹⁰ In addition, Dubicki and Martin¹¹ have characterized the diffuse-reflectance spectrum for dirhodium(II) tetraacetate dihydrate, and a plot for the rhodium(II) isobutyrate was presented in this reference. An aqueous solution spectrum in the UV region down to 200 nm was also presented.

Experimental Section

Rhodium(II) acetate was prepared from rhodium(III) chloride by the method of Rempel et al.¹² and converted to the hydrate by recrystallizing from water.⁹

The procedure for recording crystal spectra has been described previously.¹³

Bulk samples of $Rh_2(O_2CCH_3)_4 \cdot 2H_2O$ were very dark green, nearly black. A number of crystals had the form of thin platelets with well-defined faces. The extinctions for these faces were observed between crossed polarizers of a polarizing microscope. It was noted that the crystals were distinctly dichroic. For one extinction the color was a blue-green (bg), whereas for the other extinction the color was a yellow-green (yg). A crystal plate was found which would stand on edge so its thickness could be measured by a calibrated scale in the microscope eyepiece. Its thickness was $32 \pm 3 \mu m$. This crystal was mounted over a pinhole, and the polarized spectra shown in Figure 1 were recorded from ca. 580 to 325 nm for room temperature and with liquid helium in the cryostat. Since the cooling was by conduction, and the temperature of the sample could not be measured, the temperature has been assigned, conservatively it is believed, as 15 K.

After the spectra were recorded, this crystal was cemented to a glass fiber which was mounted on the goniometer head of a four-circle diffractometer. Ten reflections were obtained from oscillation photographs and refined. From these reflections the cell parameters were calculated by standard programs to be $a:b:c = 13.25:8.59:13.97$ and $\alpha:\beta:\gamma = 90.06:117.19:89.96$. These were in excellent agreement with the reported parameters for a monoclinic cell⁹ $a:b:c = 13.287:8.608:14.042$ and $\beta = 117.23^\circ$. Various planes of the crystal were called into the diffracting position, and it was observed that the large faces of this crystal were $\bar{1}01$ planes. It was also noted that the unique monoclinic axis, b , lay in the direction of the yellow-green extinction. Accordingly, the yg extinction has been designated as $\parallel b$ and the bg extinction has been labeled as $\perp b$ for this $\bar{1}01$ face.

A second crystal was found which was much thinner than the first. Its thickness was estimated to be 5.2 μm by comparison of its peak height at ca. 23 000 cm^{-1} in the $\parallel b$ polarization with the peak of the